IL NUOVO CIMENTO **43 C** (2020) 39
DOI 10.1393/ncc/i2020-20039-x

COLLOQUIA: IFAE 2019

Precision anomalous triple gauge coupling measurements at hadron colliders

ELENA VENTURINI(*)
Physik-Department, Technische Universität München - 85748 Garching, Germany

received 8 June 2020

Summary. — We discuss the measurements of the anomalous triple gauge couplings at Large Hadron Collider focusing on the contribution of the $\mathcal{O}_{3W}$ and $\mathcal{O}_{3\tilde{W}}$ operators. These deviations were known to be particularly hard to measure due to their suppressed interference with the SM amplitudes in the inclusive processes, leading to approximate flat directions in the space of these Wilson coefficients. The prospects for the measurements of these interactions are discussed, for HL-LHC and HE-LHC, using exclusive variables sensitive to the interference terms and taking carefully into account effects appearing due to NLO QCD corrections.

1. – Introduction

The Standard Model (SM) of particle physics provides a very successful description of most of the observed phenomena, sanctioned eventually by the discovery of the Higgs boson. However there are some experimental hints and some theoretical issues suggesting that the SM is not a complete theory, but only the low energy limit of some larger scenario with new physics (NP) above a certain scale; this motivates the experimental search for new physics. Direct searches of NP are in general more model-dependent and, despite the huge effort that has been made, so far all such investigations have led to null results and many of the most commonly considered BSM models have been ruled out in large regions of their parameter spaces. In view of this, one possible strategy is to analyse experimental data in a more model-independent way, trying to understand the real pressure that they impose on any UV completion of SM. This means to perform a general study of precision measurements, looking for deviations from SM, and to describe any new physics effect making as few assumptions as possible about the specific UV completion. The language of the SM Effective Field Theory (SMEFT) provides a well-defined organising principle for characterising the various deviations from the SM Lagrangian, given the (at least

(*) E-mail: elena.venturini@tum.de

moderate) mass gap existing between the EW scale and the NP scale Λ. As is well known, in this language the new interactions are expressed as a series of higher-dimensional operators so that the effective Lagrangian, if lepton number is conserved, can be written as $\mathcal{L}_{\rm SMEFT} = \mathcal{L}_{\rm SM} + \mathcal{L}_6 + \cdots$, where $\mathcal{L}_i = \sum_i \frac{c_i O_i}{\Lambda^{i-4}}$ and c_i are the Wilson coefficients of the operators O_i, built out from SM fields. One of the main goals of the current and High-Luminosity program of the LHC (HL-LHC), as well as of future High Energy options (HE-LHC), is the precise determination of the c_i coefficients. The main objective of [1] is the study for the measurement of two dimension-six operators affecting the triple gauge coupling among EW gauge bosons, namely

$$O_{3W} = -\frac{1}{\Lambda^2}\frac{g}{3!}\epsilon_{abc}W^{a,\mu\nu}W^{b}_{\nu\lambda}W^{c\lambda}_{\mu}, \qquad O_{3\tilde{W}} = -\frac{1}{\Lambda^2}\frac{g}{3!}\epsilon_{abc}\tilde{W}^{a,\mu\nu}W^{b}_{\nu\lambda}W^{c\lambda}_{\mu}, \tag{1}$$

where g and $W_{\mu\nu}$ are the $SU(2)_L$ gauge coupling constant and the field strength tensor and $\tilde{W}^{\mu\nu}$ its dual, $\tilde{W}^{\mu\nu} = \frac{1}{2}\epsilon^{\alpha\beta\mu\nu}W_{\alpha\beta}$. It is well known that the measurement of the Wilson coefficient of the two operators of eq. (1) is extremely challenging since the interference between the SM and NP contributions to diboson production in $2 \to 2$ scattering is suppressed in the high-energy regime as a consequence of certain helicity selection rules [2,3]. This makes it hard to precisely determine the magnitude of the c_{3W} and $\tilde{c}_{3W}$ Wilson coefficients, as well as to measure their sign and to differentiate amongst their two different contributions to the scattering amplitudes. Based on the fact that the helicity selection rules of [3] are only valid for $2 \to 2$ scattering, various observables built out from the decay products of the diboson final states have been proposed in [4,5]. These observables help to overcome the non-interference problem ensuring a larger sensitivity to the Wilson coefficient of the operators of eq. (1).

In [1] the O_{3W} and $O_{3\tilde{W}}$ operators are analysed by considering both the $pp \to WZ$ and $pp \to W\gamma$ diboson processes, carefully treating QCD next-to-leading-order (NLO) effects, which are important since they partially restore the interference between the SM and BSM amplitudes. Interestingly, it turns out that some of the selection cuts which are necessary to suppress reducible QCD background processes automatically lead to a partial restoration of the interference also at LO, an extremely relevant effect previously overlooked.

2. – Interference suppression and its restoration

Generically, the scattering cross section for any $2 \to 2$ process in the presence of higher-dimensional beyond the SM (BSM) operators can be written as

$$\sigma \sim \frac{g^4_{\rm SM}}{E^2}\Bigg[\overbrace{\left(a_0^{\rm SM} + a_1^{\rm SM}\frac{M^2}{E^2} + \cdots\right)}^{\rm SM^2} + \overbrace{\frac{E^2}{\Lambda^2}\left(a_0^{\rm int} + a_1^{\rm int}\frac{M^2}{E^2} + \cdots\right)}^{\rm BSM_6 \times SM} + \overbrace{\frac{E^4}{\Lambda^4}\left(a_0^{\rm BSM} + a_1^{\rm BSM}\frac{M^2}{E^2} + \cdots\right)}^{{\rm BSM_6}^2}\Bigg], \tag{2}$$

where E is the typical energy of the process, M is the mass of the SM particles and ellipses stand for the smaller terms in the $\left(\frac{M^2}{E^2}\right)$ expansion. In the high energy limit $E \gg M$

the leading contribution comes from the $a_0^{\rm SM,int,BSM}$ terms in the brackets corresponding to the massless limit of the SM particles. In [3] it was shown that $a_0^{\rm int}$ (the leading contribution to the interference term) is equal to zero for all of the processes containing transversely polarised vector bosons. This effect comes from the fact that the SM and NP amplitudes contain transverse vector bosons in the different helicity eigenstates. Dramatically, this interference suppressions implies that the high-energy measurements of the Wilson coefficients will not benefit from the usual growth of the amplitudes with the energy expected from dimension-six operators. This negatively affects the possibilities of high-energy hadron colliders, where the strongest bounds can usually be obtained by exploiting the relative enhancement of the NP contribution compared to the SM one in the high-energy distribution tails (see also [6-9]).

2˙1. *Modulation from azimuthal angle differential distributions.* – For concreteness let us consider the process $qq \to V_T V_T$, where $V = W^\pm, Z, \gamma$ and we will always work in the high energy limit, $E \gg m_V$. In the SM then the only amplitudes that will be generated at leading order in energy are $A_{\rm SM}(q\bar{q} \to V_{T,\pm} V_{T,\mp})$, where the helicities of the final state vector bosons are explicitly indicated. At the same time the dimension-six operators in eq. (1) generate only the amplitudes $A_{\rm BSM}(q\bar{q} \to V_{T,\pm} V_{T,\pm})$. Clearly, there is no interference between the BSM and SM contributions. This is the core of the above mentioned helicity selection rules. However note that at least one of the vector bosons in the final state is not stable. Hence the physical process is not a $2 \to 2$ but instead a $2 \to 3$ or $2 \to 4$ scattering. For simplicity let us consider the case of $q\bar{q} \to W_T \gamma$ with a leptonically decaying W. In the narrow width approximation the leading contribution to the interference, *i.e.*, the cross term SM $\times$ BSM in the differential cross section, summing over the intermediate polarisations of the on-shell W, is given by

$$\frac{\pi}{2s}\frac{\delta(s-m_W^2)}{\Gamma_W m_W}\mathcal{M}^{\rm SM}_{q\bar{q}\to\gamma_+ W_{T_-}}(\mathcal{M}^{\rm BSM}_{q\bar{q}\to\gamma_+ W_{T_+}})^*\mathcal{M}_{W_{T_-}\to l_-\bar{\nu}_+}\mathcal{M}^*_{W_{T_+}\to l_-\bar{\nu}_+} + \text{h.c.}. \tag{3}$$

A simple calculation shows that

$$\mathcal{M}_{W_{T_-}\to l_-\bar{\nu}_+}\mathcal{M}^*_{W_{T_+}\to l_-\bar{\nu}_+} \propto e^{-2i\phi}, \tag{4}$$

where ϕ is the angle spanned by the plane of the W decay products and the $W\gamma$ scattering plane. As shown in [1, 5], the phase of the expression $\mathcal{M}^{\rm SM}_{q\bar{q}\to\gamma_+ W_{T_-}}(\mathcal{M}^{\rm BSM}_{q\bar{q}\to\gamma_+ W_{T_+}})^*$ can be identified using the optical theorem and its properties under CP transformations and is such that

$$\mathcal{M}^{\rm SM}_{q\bar{q}\to\gamma_+ W_{T_-}}(\mathcal{M}^{\rm BSM}_{q\bar{q}\to\gamma_+ W_{T_+}})^* = \eta_{CP}(\text{BSM})[\mathcal{M}^{\rm SM}_{\rm q\bar{q}\to\gamma_+ W_{T_-}}(\mathcal{M}^{\rm BSM}_{\rm q\bar{q}\to\gamma_+ W_{T_+}})^*]^*. \tag{5}$$

By using the results in eq. (5) and eq. (4), one can see that the differential cross sections from the SM$\times$BSM interference arising from the insertion of the O_{3W} and $O_{3\tilde{W}}$ operators have the following form:

$$\begin{aligned} &O_{3W}\colon \mathcal{M}_{W_{T_-}\to l_-\bar{\nu}_+}\mathcal{M}^*_{W_{T_+}\to l_-\bar{\nu}_+} + \text{h.c.} \propto \cos(2\phi_W),\\ &O_{3\tilde{W}}\colon \mathcal{M}_{W_{T_-}\to l_-\bar{\nu}_+}\mathcal{M}^*_{W_{T_+}\to l_-\bar{\nu}_+} - \text{h.c.} \propto \sin(2\phi_W). \end{aligned} \tag{6}$$

Similar arguments can be applied to the case of WZ production. There, since only one pair of the intermediate vector bosons have opposite helicities, the modulation factorises

into a sum of two independent terms and reads

$$O_{3W}\colon\ \propto \cos(2\phi_W) + \cos(2\phi_Z), \qquad O_{3\tilde{W}}\colon\ \propto \sin(2\phi_W) + \sin(2\phi_Z). \tag{7}$$

The take home message is that by exploiting the modulations of eq. (6) and eq. (7) it is possible to increase the precision on the determination of the Wilson coefficients associated with the O_{3W} and $O_{3\tilde{W}}$ operators by overcoming the suppression of the interference terms of the cross section, suppression that is recovered with no ambiguity by performing a complete integration over the ϕ_i angles.

So far, an ideal situation has been taken into account, assuming that the azimuthal angles can be exactly determined. However, the azimuthal angle determination suffers from a twofold degeneracy as pointed out in [5]. In the case of the Z boson we cannot unambiguosly identify the helicities of the final state leptons. Since the orientation of the vector decay plane is defined considering the helicities of the final fermions, this translates into the ambiguity $\phi_Z \leftrightarrow \phi_Z - \pi$. None of the modulations of eq. (7) are however affected by this, since they are functions of $2\phi_Z$. In the case of W boson decay, differently than for the Z boson, the helicities of the final state leptons are fixed by the pure left-handed nature of the EW interactions. However, the azimuthal angle determination suffers from a twofold ambiguity on the determination of the longitudinal momentum of the invisible neutrino, arising from the quadratic equation determining the on-shellness of the W boson, as discussed in [1, 5]. All together for boosted W bosons this leads to the approximated ambiguity $\phi_W \to \pi - \phi_W$. This clearly washes away the $\sin(2\phi_W)$ modulations of eq. (6) and eq. (7).

2˙2. *Modulation from kinematic cuts.* – A partial restoration of the interference between the SM and the BSM amplitudes arises also from the imposition of certain kinematic cuts. Let us consider for example the cut, imposed in the experimental analysis [10], on the W boson transverse mass which is defined as $(M_W^T)^2 = (p_T^e + \not{p}_T)^2 - (\vec{p}_T^{\,e} + \vec{\not{p}}_T)^2$, where $\vec{\not{p}}_T \approx \vec{p}_T^{\,\nu}$. As pointed out in [1], there is a strong correlation between this variable and ϕ_W. In particular, a small M_W^T is in correspondence with a value of 0 or π for ϕ_W, while, for large p_T^γ, a cut on the W boson transverse mass automatically selects events in the azimuthal bin $[\pi/4, 3\pi/4]$. These two behaviors can easily be understood analytically.

Indeed, in the limit $M_W^T \sim 0$ the transverse momenta of the decay products of the W boson are parallel, which is to say $\vec{p}_T^{\,e} \parallel \vec{p}_T^{\,\nu} \parallel \hat{a}$, where $\hat{a}$ is a unit vector in the transverse plane. Then, the normals to the scattering plane and the decay planes are parallel, since $\vec{n}_{\text{decay}} \propto \vec{p}_\nu \times \vec{p}_e \propto \vec{p}_W \times \vec{p}_e \parallel \hat{a} \times \hat{z}$ and $\vec{n}_{\text{scat.}} \propto \vec{p}_W \times \hat{z} \parallel \hat{a} \times \hat{z}$, where $\hat{z}$ is a unit vector parallel to the beam line. Thus, the azimuthal angle can only take the values of 0 or π.

Furthermore, in the high-energy regime one can also understand the correlation between M_T^W and ϕ_W in the $M_T^W \sim M_W$ limit. Indeed, if the W boson is strictly on shell, then the condition $M_T^W = M_W$ leads to $\frac{|\vec{p}_T^{\,e}|}{|\vec{p}_T^{\,\nu}|} = -\frac{p_z^e}{p_z^\nu}$. This condition, in the limit $p_T^W \gg p_z^W$, which is equivalent to require $p_T^\gamma \gg p_z^\gamma$, forces $p_T^{e,\nu} \gg p_z^{e,\nu}$. Hence in this case the normal to the decay plane will be always along the $\hat{z}$-direction, so that the azimuthal angle will take a value equal to $\pi/2$. Then, we see that a high M_T^W cut, together with the requirement of a large photon transverse momentum, lead to the automatic selection of a preferred azimuthal angle bin. In the analysis performed in the following, the events are binned in function of the transverse mass of the $W\gamma$ system; however for a $2 \to 2$ scattering there is a one-to-one correlation between the W boson and the photon transverse momenta. Hence, by selecting bins with high $m_{W\gamma}^T$ we automatically select events with high p_T^γ which, as shown above, lead to the selection of events where $\phi_W \sim \pi/2$.

It is important to stress that a cut on the W boson transverse mass that has been discussed is imposed in the experimental analysis of [10], considered in [1]. This kinematic selection is used to suppress backgrounds arising from processes without genuine missing transverse momentum, such as the overwhelming QCD γj background where a jet is misidentified as a lepton. Hence this *modulation from cuts* behavior is always present when performing a real experimental analysis. This is an important effect which has been overlooked in similar studies in the previous literature and that leads to an enhanced sensitivity with respect to what is naively expected. A similar effect also occurs in WZ channel process; however quantitatively it turns out to be less important than in the $W\gamma$ case.

3. – $pp \to WZ$ and $pp \to W\gamma$ analysis

The hard scattering fully leptonic $pp \to WZ, W\gamma$ processes is simulated via the `MadGraph5_aMCNLO` platform [11]; the BSM operators $\mathcal{O}_{3W}$ and $\mathcal{O}_{3\tilde{W}}$ are turned on using the `HELatNLO_UFO` model that have been implemented in the `FeynRules` package [12] and exported under the `UFO` format [13] by the authors of [14]. The study is performed at NLO in QCD; parton showering and hadronisation of partonic events has been performed with `PYTHIA8` [15]. The discussion that follows refers to the analysis shown in [1], in which further details about simulations, tools, backgrounds, reconstruction efficiencies and systematic errors are provided and where the study of detector smearing effects on angular variables is presented.

The processes, in the leptonic decay channel, are considered separately for the two W boson charge signs, at NLO for the LHC with a center-of-mass energy of 14 TeV. The same cuts and requirements as in the experimental analyses of [16] and [10] are imposed, respectively, for $pp \to WZ$ and $pp \to W\gamma$. In particular, in the latter, $M_T^W > 70\,\text{GeV}$ is required, that, as mentioned, strongly suppresses the backgrounds from processes without genuine missing transverse energy. The events are categorised with respect to four angular ϕ_Z bins (in the case of WZ production) and two ϕ_W bins, equally spaced in the range 0 to π, and with respect to the WZ and $W\gamma$ system transverse masses (see [1]). Bounds on the Wilson coefficients c_{3W} and $c_{3\tilde{W}}$ are set expressing the cross section, in the presence of the two EFT operators, as

$$\sigma = \sigma_0 + \sigma^{\text{int}} c_{3W} + \tilde{\sigma}^{\text{int}} \tilde{c}_{3W} + \sigma^{\text{BSM}_1} c_{3W}^2 + \sigma^{\text{BSM}_2} \tilde{c}_{3W}^2 + \sigma^{\text{BSM}_3} c_{3W} \tilde{c}_{3W}. \tag{8}$$

Binning the events with respect to ϕ_Z, ϕ_W and $m^T_{WZ,W\gamma}$, the 95% posterior probability limits on c_{3W} and $\tilde{c}_{3W}$ are computed, fixing a maximum value of 1500 GeV for $m^T_{WZ,W\gamma}$, for an integrated luminosity of $3000\,\text{fb}^{-1}$, *i.e.*, at the end of the high-luminosity phase of the LHC. In fig. 1 there are the 68% and 95% limits in the c_{3W}-$\tilde{c}_{3W}$ plane obtained from WZ (left) and $W\gamma$ (right) production, assuming the SM (first and third panels) or a signal injection with $c_{3W} = \tilde{c}_{3W} = 0.4\,\text{TeV}^{-2}$ in the WZ case (second panel) and $c_{3W} = -\tilde{c}_{3W} = 0.3$ for $W\gamma$ (fourth panel). There the black and red curves correspond to the probability contours with and without the azimuthal binning and the shaded areas in the first and third panels correspond to the bounds derived from the non-observation of a neutron (dark blue) and electron (light blu) EDM (see [1]). Notice that in the case of $W\gamma$ production, we can only restore the interference for the CP-even operator, due to the ambiguity in the W boson decay azimuthal angle.

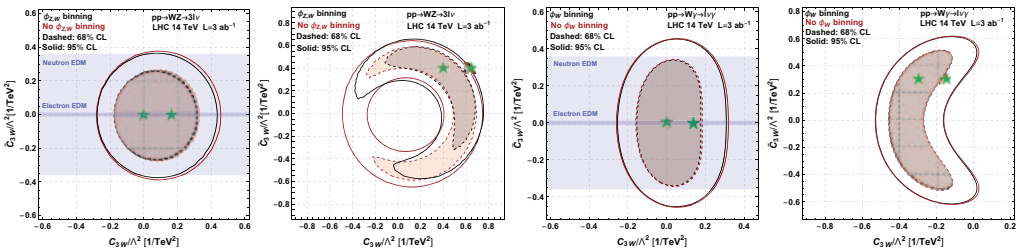

Fig. 1. – 68% (dashed) and 95% (solid) posterior probability contours for the analysis with (black) and without (red) the binning in the azimuthal angles. The two left plots refer to $pp \to WZ$ analysis, the two on the right to $pp \to W\gamma$. The first and third plots are obtained assuming the SM, the second and fourth with BSM signals with $c_{3W} = \tilde{c}_{3W} = 0.4$ and $c_{3W} = -\tilde{c}_{3W} = 0.3$, all represented by a green star. The shaded blue correspond to the limits obtained by the non-observation of a neutron and electron EDM (see [1]). Only events with $m^T_{WZ,W\gamma} < 1.5\,\text{TeV}$ are used.

We observe that the use of the azimuthal variables marginally improves the limits when the SM is assumed. This comes from the combination of three different effects. Firstly, we are considering both the linear and the quadratic term in the EFT expansion, where the latter is not affected from the helicity selection rule cancellation and is not enhanced by the kind of angular binning used here to resurrect the interference term. It turns out that in the case of WZ production at 14 TeV the quadratic contribution to bounds has similar size with respect to the one from the resurrected interference, differently to what happens for HE-LHC at 27 TeV and in the case of $W\gamma$ productions, where the linear term is dominant. Secondly the helicity selection rules are violated by QCD NLO effects and thus the resurrection of a non-vanishing interference is present even without angular differential distribution. Lastly, the imposition of kinematic cuts to select the analysis signal region has also the effect of restoring the interference between the SM and the BSM amplitude: in sect. **2**˙2 it has been shown that the cut on M_T^W, in combination with a high p_T of the W, automatically selects the value of the W decay

TABLE I. – *Summary of the results for the various channels in terms of the CP-even and CP-odd anomalous triple gauge couplings. Only events with* $m^T_{WZ,W\gamma} < 1.5$ *TeV are used.*

Channel	Energy	Luminosity	λ_Z [$\times 10^{-3}$]		$\tilde{\lambda}_Z$ [$\times 10^{-3}$]	
			68%	95%	68%	95%
WZ	14 TeV	3 ab^{-1}	[−2.1, 1.2]	[−2.9, 1.7]	[−1.7, 1.7]	[−2.4, 2.4]
	27 TeV	3 ab^{-1}	[−1.4, 0.7]	[−2.2, 1.2]	[−1.5, 1.3]	[−2.0, 1.8]
		15 ab^{-1}	[−0.7, 0.4]	[−1.2, 0.6]	[−0.9, 0.8]	[−1.3, 1.2]
$W\gamma$	14 TeV	3 ab^{-1}	[−1.2, 0.9]	[−2.0, 1.6]	[−2.2, 2.1]	[−3.0, 2.9]
	27 TeV	3 ab^{-1}	[−0.7, 0.4]	[−1.2 0.8]	[−1.8, 1.7]	[−2.5, 2.4]
		15 ab^{-1}	[−0.4, 0.2]	[−0.6, 0.3]	[−1.3, 1.2]	[−1.7, 1.5]

azimuthal angle to be close to $\pi/2$. This effect is stronger for the $W\gamma$ process, in which the M_T^W cut is harder.

However, one can notice that, in the case of WZ production, the use of the azimuthal angles is crucial in the case of a signal discovery at the LHC. As illustrated in the second and fourth panel of fig. 1 these variables can in fact be used to disentangle the contribution of the O_{3W} and $O_{3\tilde{W}}$ operators as well as to measure the sign of both the Wilson coefficients. In the analysis of $pp \to W\gamma$, the strong sensitivity to the CP-even interference term allows us to determine the sign of c_{3W}, even without inserting explicitly the azimuthal binning, due to the *modulation from cuts* effect.

4. – Summary

An analysis of diboson production, $pp \to WZ$ and $pp \to W\gamma$, is performed at NLO QCD order in the presence of the dimension-six operators of eq. (1), paying a particular attention to the effects related to the interference between the SM and BSM contributions. It turns out that NLO QCD effects mildly affects the results of the analogous LO analysis, in [4], since the helicity selections rules do not apply at NLO. For both the $pp \to WZ$ and $pp \to W\gamma$ processes the observables related to the azimuthal angles lead to an enhancement of the interference providing a better sensitivity to the new physics interactions. Interestingly, some of the kinematic selection cuts needed to suppress the reducible backgrounds in realistic analyses are partially performing an azimuthal angular bin selection, particularly for the $pp \to W\gamma$ processes. In table I, the prospects of the bounds on the triple gauge couplings λ_Z and $\tilde{\lambda}_Z$ (normalized as $O_{\lambda_Z} = \lambda_Z \frac{ig}{m_W^2} W^{+\mu_2}_{\mu_1} W^{-\mu_3}_{\mu_2} W^{3\mu_1}_{\mu_3}$ and analogously for $\tilde{\lambda}_Z$) at the HL and HE phases of the LHC are presented.

REFERENCES

[1] Azatov A., Barducci D. and Venturini E., *JHEP*, **04** (2019) 075, arXiv:1901.04821 [hep-ph].

[2] Dixon L. J. and Shadmi Y., *Nucl. Phys. B*, **423** (1994) 3; *Nucl. Phys. B*, **452** (1995) 724(E), arXiv:hep-ph/9312363.

[3] Azatov A., Contino R., Machado C. S. and Riva F., *Phys. Rev. D*, **95** (2017) 065014, arXiv:1607.05236 [hep-ph].

[4] Azatov A., Elias-Miro J., Reyimuaji Y. and Venturini E., *JHEP*, **10** (2017) 027, arXiv:1707.08060 [hep-ph].

[5] Panico G., Riva F. and Wulzer A., *Phys. Lett. B*, **776** (2018) 473, arXiv:1708.07823 [hep-ph].

[6] Baur U., Han T. and Ohnemus J., *Phys. Rev. D*, **51** (1995) 3381, arXiv:hep-ph/9410266.

[7] Falkowski A., Gonzalez-Alonso M., Greljo A., Marzocca D. and Son M., *JHEP*, **02** (2017) 115, arXiv:1609.06312 [hep-ph].

[8] Franceschini R., Panico G., Pomarol A., Riva F. and Wulzer A., *JHEP*, **02** (2018) 111, arXiv:1712.01310 [hep-ph].

[9] Grojean C., Montull M. and Riembau M., *JHEP*, **03** (2019) 020, arXiv:1810.05149 [hep-ph].

[10] CMS Collaboration (Chatrchyan S. *et al.*), *Phys. Rev. D*, **89** (2014) 092005, arXiv:1308.6832 [hep-ex].

[11] Alwall J. *et al.*, *JHEP*, **07** (2014) 079, arXiv:1405.0301 [hep-ph].

[12] Alloul A., Christensen N. D., Degrande C., Duhr C. and Fuks B., *Comput. Phys. Commun.*, **185** (2014) 2250, arXiv:1310.1921 [hep-ph].

[13] Degrande C., Duhr C., Fuks B., Grellscheid D., Mattelaer O. and Reiter T., *Comput. Phys. Commun.*, **183** (2012) 1201, arXiv:1108.2040 [hep-ph].
[14] Degrande C., Fuks B., Mawatari K., Mimasu K. and Sanz V., *Eur. Phys. J. C*, **77** (2017) 262, arXiv:1609.04833 [hep-ph].
[15] Sjostrand T., Mrenna S. and Skands P. Z., *Comput. Phys. Commun.*, **178** (2008) 852, arXiv:0710.3820 [hep-ph].
[16] The ATLAS Collaboration, ATLAS-CONF-2018-034.